Desalination and Water Treatment
www.deswater.com

doi: 10.5004/dwt.2023.29375

291 (2023) 170–181
April

Recyclable green hydrogel adsorbents with excellent adsorption capacity for removal of methylene blue

Yanqin Xu†, Biemin Sun†, Yuan Cao*, Changguo Chen*

College of Chemistry and Chemical Engineering, Chongqing University, Chongqing 401331, China, Tel.: +86 15923344273; email: caoyuan@cqu.edu.cn (Y. Cao), Tel.: +86 13608357956; emails: cgchen@cqu.edu.cn (C. Chen), xuyanqin666@163.com (Y. Xu), 1025577487@qq.com (B. Sun)

Received 18 November 2022; Accepted 20 February 2023

ABSTRACT

The recyclable green carboxymethyl chitosan-oxidized sodium alginate-gelatin/polyacrylamide double network hydrogel was simply and rapidly synthesized by one-pot method. This hydrogel with satisfactory mechanical properties was used to adsorb methylene blue, showing a high adsorption capacity, recyclability and environmental friendliness. The results showed that the adsorption of methylene blue solution (50 mL of 50 mg·L^{-1}) with 15 mg of adsorbent resulted in a removal rate of over 93%, and the adsorption rate was still over 86% after 7 adsorption–desorption cycles. The adsorption of methylene blue by hydrogel adsorbents was consistent with the Langmuir adsorption isotherm model and pseudo-second-order kinetic adsorption process, mainly through electrostatic and hydrogen bonding interactions. In this work, the prepared hydrogels have a high adsorption capacity and stable cycle adsorption–desorption, which are beneficial to the application in the purification of dye wastewater.

Keywords: Double network hydrogel; Dye wastewater; Adsorbent; Adsorption kinetics; Adsorption isotherms

---

1. Introduction

With the expansion of the scale of textile, printing and dyeing industry [1–3], the resulting of dye wastewater has also been increasing. Water environment and human health are seriously affected by the pollution caused by organic dye wastewater [4], if discharged directly into natural water without treatment, it will lead to the death of aquatic organisms. Under certain conditions, azo dyes can produce a variety of carcinogenic aromatic amines [5], threatening human life and health. How to improve the treatment effect of dye wastewater has become the focus of researchers. Many strategies such as biocatalytic degradation [6,7], adsorption [8], membrane separation [9,10] electrochemistry [11] and chemical oxidation [12,13] have been used to treat wastewater contaminated by organic dyes. Among them, adsorbents have been widely used in the treatment of organic dye wastewater due to their wide variety, recyclability and high efficiency.

As a new type of adsorbent, hydrogels [14–16] have a three-dimensional network structure, high porosity, recyclability and simple synthesis process. Hydrogels based on natural biomass [17–19], such as gelatin, chitosan, sodium alginate and cellulose, have rich active groups such as hydroxyl (–OH), amino (–NH$_2$) and carboxyl (–COOH) groups, which can realize the reversible adsorption–desorption of dye molecules. For example, Ren et al. [20] successfully synthesized a biodegradable porous green adsorbent hydrogel, which can effectively adsorb methylene blue. When the concentration of methylene blue was 30 mg·L^{-1}, the removal rate was between 80.0% and 93.3%. Wang et al. [21] prepared carboxymethyl cellulose/chitosan

---

* Corresponding authors.

† These authors contributed equally to this work.

1944-3994/1944-3986

interpenetrating network hydrogel for adsorption–desorption of anionic and cationic dye. Under the optimized conditions, the adsorption capacity and desorption rate of methylene blue were still high after 5 adsorption–desorption cycles. Sodium alginate is a linear polyhydroxy natural polymeric polysaccharide found in brown algae [22], which is widely available, cost effective and environmentally friendly [23]. Sodium alginate is rich in carboxyl and hydroxyl groups, which can bind to dye molecules and is used to remove dye contamination from water. The combination of sodium alginate and other polymers can enhance water pollutant removal properties, and the introduction of inorganic materials, which can also remove pollutants by ion exchange or adsorption. Kausar et al. [24] successfully prepared a cellulose/clay/sodium alginate composite, which proved to be a low-cost alternative adsorbent for the decontamination of dye contamination, achieving 90% dye adsorption under optimal adsorption conditions. Moderate grafting modification of sodium alginate can enhance its adsorption capacity, and covalent or non-covalent cross-linking can change chemical resistance and mechanical strength. Wang et al. [25] synthesized sodium alginate grafted polymer composite beads, which had a special cross-linked network structure and abundant functional groups and showed excellent adsorption performance for the dye methylene blue, with the adsorption capacity of 390.78 $mg \cdot g^{-1}$ for methylene blue. Soury et al. [26], successfully prepared mesoporous tetrakis(2,4,6-trimethylphenyl)porphyrin zinc(II)-loaded sodium alginate gel beads, and the maximum adsorption capacity of sodium alginate composite beads for methylene blue was 52.3 $mg \cdot g^{-1}$. In order to, overcome the limitations of sodium alginate in wastewater treatment due to its mechanical defects. Kondaveeti et al. [27], synthetized alginate/xanthan co-blended beads and freeze-dried them in calcium chloride to improve the porosity. 91% removal of methylene blue was still achieved by the beads after 4 adsorption–desorption cycles. For the improvement of the adsorption capacity of the sodium alginate adsorbent, other substances can be introduced to compound and chemically modify it. The improved mechanical properties facilitate better applications in water treatment. For the treatment of organic dye wastewater, recyclable green hydrogel has the advantages [28–30] of low price, wide source range, biodegradability, and environmentally friendly. However, their practical application in industry is limited due to low adsorption capacity, poor mechanical property and stability [31,32].

Double network hydrogel [33–35] is a composite material whose mechanical property and stability can be greatly improved due to the introduction of another network. Polyacrylamide (PAM) has been used to remove various metal ions and dyes from aqueous solutions [36] with many advantages such as biodegradability, hydrophilicity, and adsorption property. The double network hydrogel is obtained by introducing polyacrylamide network into the biomass-hydrogel network, which can not only improve its mechanical property and stability, but also improve its adsorption performance. Yao et al. [37], prepared magnetic polyacrylamide porous microspheres for adsorbing cationic dyes, the results showed that the microspheres had high adsorption efficiency for methylene blue, and the adsorption capacity increased from 263 to 1,977 $mg \cdot g^{-1}$, as the initial methylene blue concentration increased from 5 to 300 $mg \cdot L^{-1}$. Maijan et al. [38], developed a hydrogel (NR-*g*-PAM) based on a semi-interpenetrating network of natural rubber and polyacrylamide. The formation of the semi-interpenetrating network structure improved the mechanical property, and the removal rate of methylene blue from the NR-*g*-PAM hydrogel was 90%. However, it is rare to use the hydrogel composited with natural biomass polymer and polyacrylamide for the treatment of dye wastewater.

In this study, we simply and quickly synthesized a carboxymethyl chitosan-oxidized sodium alginate-gelatin/polyacrylamide (CMCS-OSA-GEL/PAM) hydrogel as adsorbents with high adsorption performance, excellent mechanical properties and multiple recycling by one pot method, and evaluated its adsorption effect by adsorbing methylene blue represented organic dye wastewater. A large number of active functional groups such as hydroxyl (–OH), amino ($-NH_2$) and carboxyl (–COOH) groups beneficial to adsorption came from cheap biomass such as carboxymethyl chitosan, gelatin and oxidized sodium alginate. The Schiff base reaction of oxidized sodium alginate with gelatin and carboxymethyl chitosan was used as the first network, and the polyacrylamide obtained through free radical polymerization was used as the second network. The chemical structure, micro morphology and properties of the double network hydrogels were characterized. The effects of factors such as adsorbent dosage, initial methylene blue concentration, pH and temperature on the adsorption properties were also studied. In addition, the isotherms, kinetics and adsorption mechanism of the adsorption process were also studied.

2. Materials and methods

2.1. Materials

Gelatin (GEL, BR, molecular weight: 10,000–50,000), carboxymethyl chitosan (CMCS, BR, degree of substitution >80%,) and methylene blue (≥90%,) were purchased from Macklin, Shanghai. Sodium alginate (AR, molecular weight: 2,000–5,000, viscosity: 15–60 mpa·s), sodium periodate ($NaIO_4$, AR), acrylamide (AM, 99%), N,N′-methylene bisacrylamide, (MBA, 99%), ammonium persulfate (AR, 98.5%), N,N,N′,N′-tetramethylethylenediamine (TEMED, 99%), ethylene glycol (AR, 98%), absolute ethanol (AR) and hydrochloric acid (AR) were purchased from Chengdu Kelong Chemical Co., Ltd., (Chengdu, China). Deionized water (self-made in the laboratory).

2.2. Preparation of oxidized sodium alginate

The oxidized sodium alginate was prepared according to this literature [39]. Sodium alginate (5 g) was dispersed in 25 mL absolute ethanol in a round bottom flask, and sodium periodate (2.8 g) was dissolved in deionized water. Then the sodium periodate solution slowly was added to the round bottom flask. The reaction was stirred in a magnetic stirrer for 6 h under shading conditions. Finally, ethylene glycol (2 mL) was added slowly and stirred for 1 h to terminate the reaction. The white substance obtained from the reaction was added to ethanol, stirred and filtered, then the product was washed by a mixture of water and ethanol (1:1), filtered and repeated three times, dried in a vacuum drying oven (40°C, 12 h) to obtain a solid product.

2.3. Preparation of CMCS-OSA-GEL/PAM double network hydrogel

CMCS-OSA-GEL/PAM double network hydrogel was prepared by a simple and easy one-pot method [40]. First, OSA solution was added to GEL (8 wt.%), CMCS (4 wt.%), AM (6 wt.%), MBA (0.1 wt.%) mixed solution to stir, ultrasonic and make the first network react. After 5 min, the catalyst TEMED (40 μL) was added and mixed uniformly by ultrasonic, the initiator ammonium persulfate (1 mL, 0.3 wt.%) was added to initiate the free radical polymerization to obtain the second network, and the CMCS-OSA-GEL/PAM double network hydrogel was obtained. In order to, investigate the effect of OSA concentration on adsorption performance, CMCS-OSA-GEL/PAM double network hydrogel was prepared with different concentrations of OSA.

2.4. Characterization

The structural changes of OSA-SA were analyzed by Proton nuclear magnetic resonance (^{1}H NMR; JNM-AL400, JEOL Co., Ltd., Japan). The functional groups of OSA and CMCS-OSA-GEL/PAM hydrogel were analyzed by Fourier-transform infrared spectroscopy (Nicolet iN10, Thermo Fisher, USA). The pore structure of CMCS-OSA-GEL/PAM hydrogel was observed by scanning electron microscope (JSM-6490LV FEI). Zeta potential of the sample was measured by using the Marvin laser particle size analyzer. The compressive strength of the double network hydrogel was tested by a universal material testing machine (Shimadzu AG-Xplus, Japan) at a pressing speed of 8 mm/min, the size of the hydrogel was a cylinder with a diameter of 15 cm and a height of 10 cm.

2.5. Determination of swelling properties of CMCS-OSA-GEL/PAM hydrogel

The swelling properties of CMCS-OSA-GEL/PAM hydrogel were determined by gravimetric method. After recording the initial weight of the freeze-dried hydrogel, it was immersed in excess deionized water. The hydrogel was taken out and weighed at regular intervals. Repeating the above steps until the hydrogel quality was almost unchanged, that was, the hydrogel had reached the equilibrium of wetting and swelling. The swelling degree of hydrogel was calculated by equilibrium swelling ratio (ESR) (g·g^{-1}) formula:

$$\text{ESR} = \frac{W_d - W_0}{W_0} \tag{1}$$

where W_d is the mass of double network gel when absorbing water for a certain time and W_0 is the mass of dry double network gel.

2.6. Adsorption properties of CMCS-OSA-GEL/PAM hydrogel

First, 1.0 g·L^{-1} methylene blue solution (0.25 g methylene blue dye, 250 mL volumetric flask) was prepared as mother liquor, diluted to different concentrations of methylene blue solutions (2, 4, 6, 8, and 10 mg·L^{-1}, respectively), and the absorbance was measured at 664.5 nm with UV-visible spectrophotometer [41] (TU-1900) to obtain the standard curve. The concentration of dye solution was measured by UV-visible spectrophotometer. 30 mL of 0.3 mol·L^{-1} hydrochloric acid solution was prepared as desorption agent. The effects of hydrogel dosage, pH, temperature and the concentration of methylene blue solution on adsorption were studied. The adsorption and desorption of the double network hydrogel were carried out in a constant temperature water bath shaker (HNY) at a speed of 100 r·min^{-1}. The adsorption capacity q (mg·g^{-1}) and the removal rate E (%) of CMCS-OSA-GEL/PAM hydrogel were calculated by the following equations:

$$q_e = \frac{\left(C_0 - C_e\right)V}{W} \tag{2}$$

$$q_t = \frac{\left(C_0 - C_t\right)V}{W} \tag{3}$$

$$E = \frac{\left(C_0 - C_e\right)}{C_e} \times 100\% \tag{4}$$

where q_e and q_t (mg·g^{-1}) are the amount of methylene blue adsorbed by CMCS-OSA-GEL/PAM hydrogel at adsorption equilibrium and a certain time, respectively. C_0, C_t and C_e (mg·L^{-1}) are the dye concentrations at initial time, a certain time and adsorption equilibrium, respectively. V (mL) is the volume of methylene blue solution. W (g) is the mass of dry hydrogel.

3. Results and discussions

3.1. Synthesis and characterization of CMCS-OSA-GEL/PAM hydrogel

The aldehyde group (–CHO) of OSA was obtained by oxidation of sodium alginate (SA) with sodium periodate [42] ($NaIO_4$), the reaction was shown in Fig. 1a. In Fig. 1d, the first network was formed by the Schiff base reaction between the aldehyde group (–CHO) of OSA and the amino group (–NH_2) of carboxymethyl chitosan (CMCS) and gelatin (GEL) to form –C=N–, which was a reversible chemical bond and hydrogen bond connection [42]. The second network was formed by radical polymerization of acrylamide (AM) monomer under the cross-linking agent (MBA) and initiator $(NH_4)_2S_2O_8$, which was composed of irreversible covalent bonds [43]. The colorless hydrogel turned blue after adsorbing methylene blue, and the color of methylene blue solution turned pale significantly, as shown in Fig. 1d, which preliminarily proved that the double network hydrogel can adsorb methylene blue. Comparing the Fourier-transform infrared spectroscopy (FTIR) spectral of SA and OSA in Fig. 1b, OSA displayed a stretching vibration peak [42] at 1,731.32 cm^{-1}, which was caused by the stretching vibration of aldehyde group (–CHO), indicating that SA had been successfully oxidized to form OSA. ^{1}H NMR also

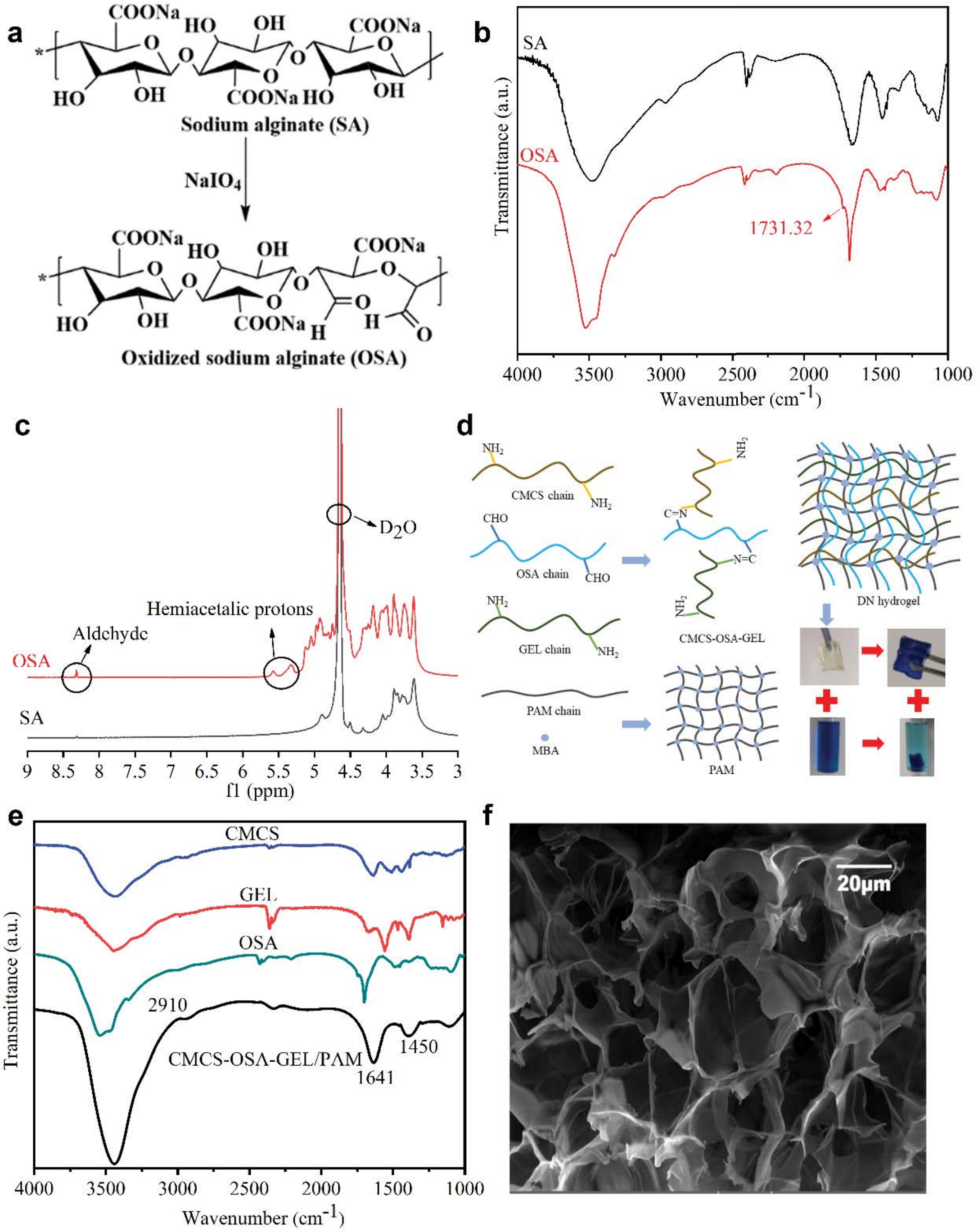

Fig. 1. Schematic diagram of the synthesis mechanism of oxidized sodium alginate (a) and double network hydrogels (d), Fourier-transform infrared spectroscopy (b) and proton nuclear magnetic resonance (c) spectra of oxidized sodium alginate, Fourier-transform infrared spectra (e) of CMCS-OSA-GEL/PAM hydrogel, and (f) scanning electron microscopy of CMCS-OSA-GEL/PAM hydrogel.

verified the FTIR results, in ^{1}H NMR of OSA in Fig. 1c, a new signal peak appeared at 8.3 ppm [44], which was the characteristic peak of aldehyde group (–CHO) on OSA. The characteristic peak appearing near 5.3 to 5.6 ppm was the characteristic absorption peak produced by the semi acetal formed between the aldehyde group and the adjacent hydroxyl group. In FTIR spectrum Fig. 1e, the peaks from 1,450 to 1,700 cm^{-1} of CMCS-OSA-GEL/PAM hydrogel was the stretching vibration peaks of amide groups in the second network, and the stretching vibration peaks [45] of amide groups was at 2,910 cm^{-1}, the peak at 1,641 cm^{-1} was presumed to be the common absorption peak of Schiff base bonds and ammonia groups in the first network. Therefore, it can be inferred that the CMCS-OSA-GEL/PAM hydrogel was successfully prepared. It can be seen from the Fig. 1f that the double network hydrogel had many pores distributed and closely arranged, and the diameter of the pore was mostly 20~40 μm. These pores can provide abundant adsorption sites for the adsorption of small organic dye molecules, which were an important condition for its excellent adsorption performance.

3.2. Swelling of CMCS-OSA-GEL/PAM hydrogel

Swelling property is the evaluation of water absorption capacity of hydrogels [45]. It can be seen from Fig. 2a that the swelling degree of CMCS-OSA-GEL/PAM hydrogel was significantly lower than that of CMCS-OSA-GEL hydrogel. After swelling equilibrium, CMCS-OSA-GEL/PAM hydrogel was about 6 g·g^{-1}, while CMCS-OSA-GEL hydrogel was about 16 g·g^{-1}. The reason was that the two networks of the double network hydrogel were intertwined, which made the network structure of the hydrogel denser and restricted the entry of water molecules into the network. The double network hydrogels prepared in the experiment had low swelling properties. If the swelling degree of adsorbent material was too high, it will adsorb a large amount of water while adsorbing dyes, which was not conducive to the adsorption.

3.3. Compressive mechanical properties of CMCS-OSA-GEL/PAM hydrogel

It can be seen from Fig. 2b that the compressive mechanical properties of CMCS-OSA-GEL/PAM hydrogel were much better than those of CMCS-OSA-GEL hydrogel. The CMCS-OSA-GEL hydrogel can withstand a stress of about 0.6 MPa, after adding a polyacrylamide network, the double-network hydrogel can withstand a stress of more than 1 MPa, whose mechanical properties were significantly improved. The double network structure can make the reversible dynamic Schiff base bond and hydrogen bond in the first network as the sacrifice when the material was subjected to force, and the internal fracture will consume internal energy [46], so that the covalent bond of the second network can withstand huge deformation.

3.4. Adsorption properties of CMCS-OSA-GEL/PAM hydrogels for methylene blue

3.4.1. Effect of OSA concentration

OSA was the macromolecular crosslinker to formed the first network, which affected the pore structure of the whole double network hydrogels, so it determined its adsorption performance to a large extent. Hydrogels (10 mg) with different OSA concentrations were added to methylene blue solution (50 mL of 50 mg·L^{-1}) to investigate their adsorption properties. As can be seen from Fig. 3a, when the OSA concentration was 6 wt.%, the maximum adsorption capacity of CMCS-OSA-GEL/PAM hydrogel for methylene blue molecules was about 218 mg·g^{-1}. With the further increase of OSA concentration, the adsorption capacity decreased. As OSA was the crosslinking agent of the first network and also was a high molecular polymer, which will significantly affect the pore size and distribution of hydrogel. If OSA was too low, the formed pores will be relatively large, which was not conducive to the adsorption of small molecule methylene blue; If the concentration of OSA was too high, the double network gel will be denser and the pore distribution will be sharply reduced, resulting in a great decrease in its adsorption performance. Therefore, the selected hydrogels with an OSA concentration of 6 wt.% were used in the experiments.

3.4.2. Effect of hydrogel dosage

In order to, analyze the effect of hydrogel dosage on adsorption performance, 5, 10, 15, 20, 30 and 40 mg of hydrogel were taken to absorb methylene blue solution (50 mL of 50 mg·L^{-1}). According to Fig. 3b, with the increase of the dosage of hydrogel, the removal rate of methylene blue by CMCS-OSA-GEL/PAM hydrogel gradually increased. When the amount of hydrogel reached 15 mg, the removal rate reached 93%. Later, the dosage of hydrogel was increased, and the removal rate was almost unchanged. The adsorption capacity of methylene blue decreased gradually from 420 to 50 mg·g^{-1}. With the increase of hydrogel dosage, the active adsorption sites increased greatly, and more methylene blue came into contact with the hydrogel, which greatly

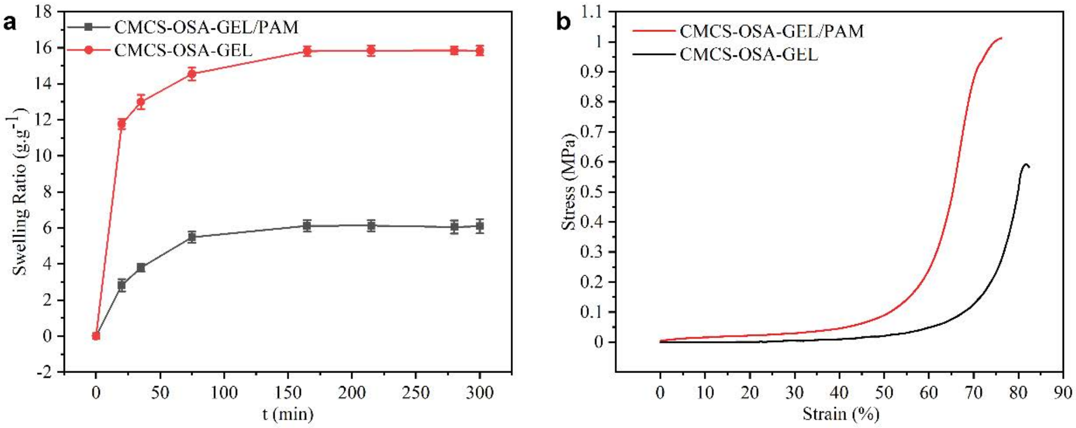

Fig. 2. (a) Swelling ratio of CMCS-OSA-GEL/PAM and CMCS-OSA-GEL and (b) compressive mechanical properties of CMCS-OSA-GEL/PAM and CMCS-OSA-GEL.

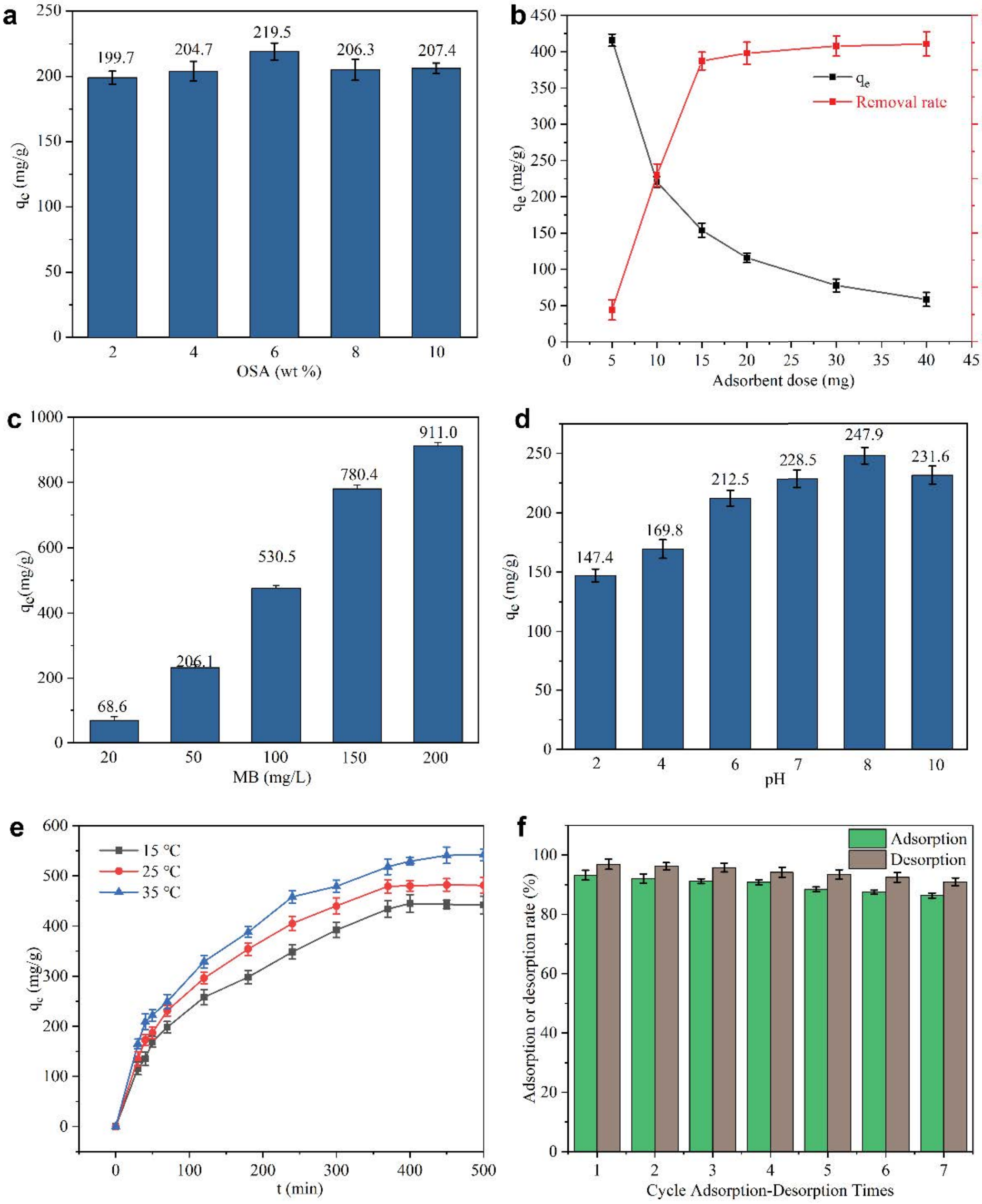

Fig. 3. Effect of oxidized sodium alginate concentration (a), adsorbent dose (b), methylene blue solution concentration (c), pH (d) and temperature (e) on the methylene blue adsorption, cycle adsorption–desorption performance (f) of CMCS-OSA-GEL/PAM hydrogel.

increased the adsorption rate. When the hydrogel dosage reached 15 mg, there were more adsorption sites, but the methylene blue molecules in the solution were limited, the adsorption was relatively saturated, more adsorption sites of hydrogel cannot be fully utilized. This result was consistent with the data reported in this literature [47].

3.4.3. Effect of methylene blue concentrations

To explore the effects of different methylene blue concentrations on the adsorption properties of CMCS-OSA-GEL/PAM hydrogel, 10 mg of hydrogel were added to methylene blue solutions with concentrations of 20, 50, 100, 150 and 200 mg·L^{-1}, respectively. From Fig. 3c, with the increase of initial methylene blue concentration, the adsorption capacity of CMCS-OSA-GEL/PAM hydrogel for methylene blue gradually increased. When the initial methylene blue concentration reached 200 mg·L^{-1}, q_e even reached 900 mg·g^{-1}. The increasing concentration difference of methylene blue will overcome the diffusion resistance between methylene blue solution and solid-phase hydrogel, making methylene blue molecules more fully contact with hydrogel, and finally improve the adsorption capacity. However, the adsorption sites of hydrogel were limited, with the increase of methylene blue concentration, the more adsorption sites occupied, the removal rate of methylene blue will decline to a certain extent. This was similar to the conclusion of this literature [48].

3.4.4. Effect of pH

CMCS-OSA-GEL/PAM hydrogel (10 mg) was added to methylene blue solution (50 mL of 50 mg·L^{-1}) whose pH was adjusted to 2, 4, 6, 8 and 10 for adsorption experiments. As shown in Fig. 3d, when the pH was 8, the adsorption capacity reached the maximum, about 247.9 mg·g^{-1}. Methylene blue was a cationic dye, which was adsorbed by hydrogel through electrostatic interaction and hydrogen bond. pH was an important factor for the adsorption process of methylene blue, which will affect its electrical property, because the hydrogel contained a large number of amino and carboxyl groups. Under acidic conditions, the $-NH_2$ group in the hydrogel network was protonated, resulting in competitive adsorption with methylene blue molecules, in addition, carboxyl groups can also be converted into carboxylic groups, which reduced the electrostatic attraction between hydrogel and methylene blue to a certain extent, resulting in the decrease of methylene blue adsorption capacity of hydrogel. When the pH > 7, the –COO– on the hydrogel surface showed a negative charge, which was conducive to the adsorption of cationic dye methylene blue [20]. Therefore, the adsorption amount of methylene blue on hydrogels had increased.

3.4.5. Effect of temperature

In order to study the effect of temperature on the adsorption performance of CMCS-OSA-GEL/PAM hydrogel, CMCS-OSA-GEL/PAM hydrogel (10 mg) was added to methylene blue solution (100 mg·L^{-1}) for adsorption experiment at 15°C, 25°C and 35°C. At certain intervals, the upper solution of methylene blue solution was taken to measure the absorbance. From Fig. 3e, the hydrogel reached adsorption equilibrium around 400 min, and its adsorption capacities were around 430, 480, and 540 mg·g^{-1} at 15°C, 25°C, and 35°C, respectively. Since the temperature increase will provide energy to accelerate the random thermal motion of the molecules, the methylene blue molecules and the CMCS-OSA-GEL/PAM hydrogel solid can be more fully contacted.

3.4.6. Cycle adsorption and desorption properties of double network hydrogels

To explore the cycle adsorption and desorption performance of CMCS-OSA-GEL/PAM hydrogel, 30 mL of 0.3 mol·L^{-1} hydrochloric acid solution was used as the desorption agent in this experiment. First, the CMCS-OSA-GEL/PAM hydrogel was saturated with methylene blue. Then, this hydrogel was put into hydrochloric acid solution and desorbed for 4 h in a constant temperature shaker at a speed of 100 rpm. From Fig. 3f, the methylene blue adsorption rate of the hydrogel decreased from 93.2% to 86.4% when cycling to the 7th time. After 7th cycle of adsorption and desorption, the removal rate of methylene blue by CMCS-OSA-GEL/PAM hydrogel still reached more than 86%, and the desorption rate was still more than 90%. This was due to the stability induced by the excellent mechanical properties of the double network hydrogel, indicating that the CMCS-OSA-GEL/PAM hydrogel was feasible as a recycling adsorption material.

3.5. Adsorption and desorption performances

3.5.1. Adsorption isotherm analysis

In this paper, Langmuir and Freundlich models were selected to describe the adsorption process [49]. The Langmuir model describes uniform energy distribution and single-layer adsorption, while the Freundlich model describes non-uniform energy distribution and multi-layer adsorption. The Langmuir and Freundlich isotherm equation are linearized into Eqs. (5) and (6), respectively:

$$\frac{C_e}{q_e} = \frac{C_e}{q_{\max}} + \frac{1}{q_{\max}K_L} \tag{5}$$

$$\ln q_e = \ln K_F + \frac{1}{n}\ln C_e \tag{6}$$

where q_e is the equilibrium adsorption capacity (mg·g^{-1}), C_e is the equilibrium concentration (mg·L^{-1}), K_L is the Langmuir isothermal constant (L·mg^{-1}) and q_m is the maximum adsorption capacity of Langmuir isotherm; K_F is related to Freundlich adsorption capacity (mg·g^{-1}(L·mg^{-1})$^{1/n}$), and the heterogeneity factor is $1/n$.

In addition, in the Langmuir adsorption isothermal model, the dimensionless separation factor R_L can also characterize whether the adsorption is favorable, which is expressed by Eq. (7):

$$R_L = \frac{1}{1+K_LC_0} \tag{7}$$

where R_L represents [50] that the adsorption process is unfavorable ($R_L > 1$); favorable ($1 > R_L > 0$); linear ($R_L = 1$); irreversible ($R_L = 0$).

Fig. 4a and b can be obtained by performing linear fitting calculation on the experimental data by Eqs. (5) and (6), respectively, which are the linear fitting diagrams of the Langmuir and Freundlich models, respectively. The data in Table 1 show that the adsorption isotherm model of hydrogel was more suitable for the Langmuir model and its correlation coefficient R^2 was higher than that of the Freundlich model. Therefore, this indicated that methylene blue was adsorbed by hydrogel as a monolayer, and separation factor R_L was also between 0 and 1, indicating that the reaction was spontaneous. Similar findings were obtained for different dye-adsorbent systems in literature [51,52]. The theoretical maximum adsorption capacity of hydrogel for methylene blue at 15°C, 25°C and 35°C were 487.8, 549.45 and 595.7 mg·g^{-1}, which was close to the experimental value.

3.5.2. Adsorption kinetic analysis

Adsorption kinetics is used to describe the change of adsorption capacity with time and to study the adsorption mechanism. Kinetic models of pseudo-first-order and pseudo-second-order represent physical and chemical adsorption, respectively [46]. For the pseudo-first-order kinetic model, the adsorption rate is mainly determined by diffusion; for the pseudo-second-order kinetic model, the interaction between adsorptions is considered to determine the adsorption rate. The pseudo-first-order and pseudo-second-order equations are represented by Eqs. (8) and (9):

$$\ln\left(q_e - q_t\right) = \ln q_e - k_1 t \tag{8}$$

$$\frac{t}{q_t} = \frac{1}{k_2 k_t^2} + \frac{t}{q_e} \tag{9}$$

where q_t is the adsorption capacity at a certain time; k_1 and k_2 is the adsorption rate constant of the pseudo-first-order and pseudo-second-order.

Fig. 5a and b are calculated by linear fitting of the experimental data through Eqs. (8) and (9), respectively, and which

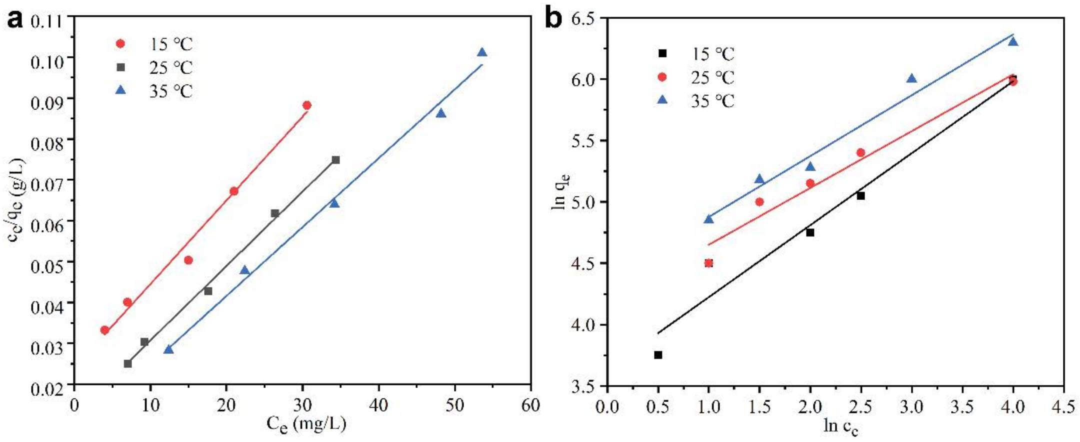

Fig. 4. Adsorption isotherm models study for methylene blue on hydrogel (a) Langmuir and (b) Freundlich adsorption isotherm.

Table 1
Langmuir and Freundlich adsorption isotherm models for the methylene blue on the hydrogel

T (K)	Langmuir				Freundlich		
	$q_{\max}$	K_L (L·mg^{-1})	R^2	R_L	K_F (mg·g^{-1}(L·mg^{-1})$^{1/n}$)	n	R^2
298	487.8000	0.00205	0.9627	0.7092	39.9600	1.7000	0.94282
308	549.4500	0.00182	0.9923	0.7331	65.8487	2.1597	0.94198
318	595.7000	0.00168	0.9928	0.7485	79.9338	2.0160	0.96916

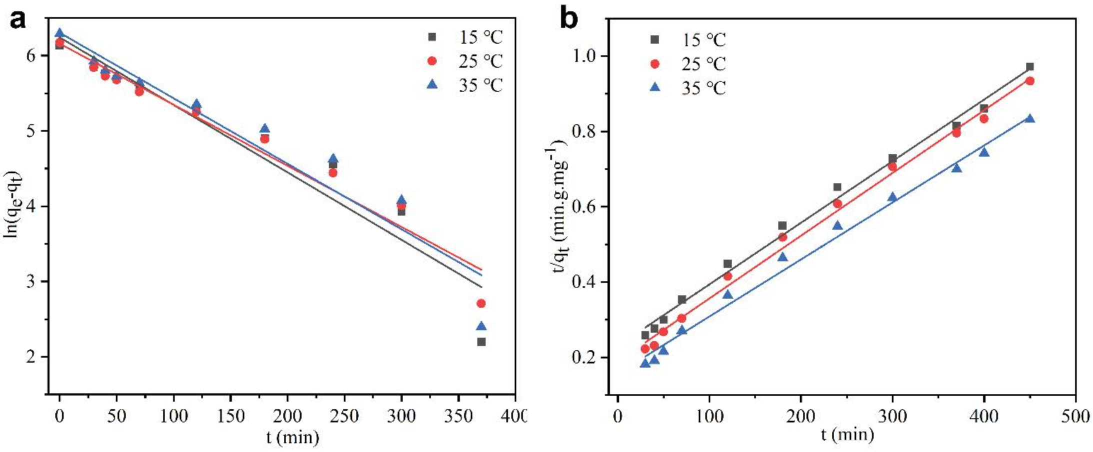

Fig. 5. Adsorption kinetic study for hydrogel pseudo-first-order (a) and pseudo-second-order (b).

are the linear fitting diagrams of pseudo-first-order (a) and pseudo-second-order (b) adsorption kinetic, respectively. According to Table 2, the correlation coefficient R^2 (>0.99) of the pseudo-second-order kinetics was higher than that of pseudo-first-order, indicating that the adsorption of methylene blue by the material was more suitable for the pseudo-second-order kinetic model. The adsorption of hydrogel was mainly chemical adsorption such as interaction between ions, hydrogen bonding, electrostatic interaction, etc.

3.5.3. Adsorption thermodynamic analysis

The exchange of energy between the environment and the system during the occurrence of adsorption is described by adsorption thermodynamics, which is also often used to observe the spontaneity and feasibility of adsorption [53]. Thermodynamic study on the process of adsorption of methylene blue (MB) in solution by double network hydrogel at 298, 308 and 318 K is carried out by using the following formulas to obtain ΔH, ΔS, ΔG.

$$K_c = \frac{K_L}{C_e} \tag{10}$$

$$\Delta G = -RT\ln K_c \tag{11}$$

$$\ln K_c = \frac{\Delta S}{R} - \frac{\Delta H}{RT} \tag{12}$$

where K_c is the equilibrium constant, K_L is Langmuir constant (L·mg^{-1}), C_e is the equilibrium concentration (mg·L^{-1}), R is the molar gas constant (8.314 J·K^{-1}·mol^{-1}), ΔG is the free energy change value (kJ·mol^{-1}) of the adsorption process, ΔH is the enthalpy change value (kJ·mol^{-1}) of the adsorption process, ΔS is the change value of the adsorption entropy (J·mol^{-1}·K^{-1}). ΔS and ΔH are obtained by using the intercept and slope of the line made by lnK_c to $1/T$.

The results show in Table 3 that $\Delta G < 0$, indicating that the adsorption of MB on the double network hydrogel was spontaneous. With the increase of temperature, the absolute value of ΔG also increased, indicating that the higher the temperature, the more favorable the adsorption of MB by the dual network hydrogel. $\Delta H > 0$ indicated that the adsorption of MB by double network hydrogels was an endothermic process. $\Delta S > 0$ meant that the whole adsorption process tended to be disorderly and spontaneous.

3.5.4. Adsorption mechanism

Methylene blue is a cationic dye. In Fig. 6a, the hydrogel adsorbent shows negative potential, after adsorption of methylene blue, the potential changed from negative potential to positive potential, indicating that the hydrogel adsorbed methylene blue through electrostatic action. At the same time, according to Fig. 6b, the –OH stretching vibration peak shifted from 3,405 to 3,384 cm^{-1}, the NH_2 stretching vibration peak shifted from 1,634 to 1,623 cm^{-1}, and the C–O stretching vibration peak shifted from 1,463 to 1,425 cm^{-1}, indicating the adsorption effect produced by the interaction between methylene blue solution and the –OH, NH_2 and C–O groups on the surface of hydrogel through hydrogen bonding and electrostatic bonding. According to Fig. 6c the nitrogen adsorption desorption isotherm before and after the adsorption of the hydrogel, the specific surface area of the hydrogel before the adsorption reaction was 0.954 m^2·g^{-1}, and after the adsorption of methylene blue, the specific surface area decreased to 0.145 m^2·g^{-1}, and the surface of the hydrogel adsorbed with methylene blue. According to the chemical structure of hydrogel, such as amino group (–NH_2), hydroxyl group (–OH) and carboxyl group (–COO–), it can be speculated that the adsorption of methylene blue was through the electrostatic interaction of ions and hydrogen bonding. methylene blue adsorption can also be achieved by pore diffusion. The adsorption of methylene blue by the hydrogel adsorbent was consistent with the Langmuir model and the pseudo-secondary kinetic model, indicating that the adsorption of methylene blue by the material was a monolayer and surface homogeneous chemisorption. The parameters of thermodynamics indicated that the adsorption reaction of the material on methylene blue was a spontaneous and heat-absorbing process.

Table 3
Thermodynamic parameters of CMCS-OSA-GEL/PAM hydrogel adsorbing methylene blue

T (K)	ΔG (kJ·mol^{-1})	ΔH (kJ·mol^{-1})	ΔS (J·mol^{-1}·K^{-1})
298	−11.05	73.74	282.68
308	−12.89		
218	−16.76		

Table 2
Adsorption kinetic parameters adsorption on CMCS-OSA-GEL/PAM hydrogel

Kinetic model	Parameters	298 K	308 K	318 K
Pseudo-first-order	k_1 (min^{-1})	8.9 × 10^{-3}	8.12 × 10^{-3}	8.7 × 10^{-3}
	q_e (mg·g^{-1})	432.11	473.43	546
	R^2	0.9188	0.9595	0.9214
Pseudo-second-order	k_2 (g·mg^{-1}·min^{-1})	1.167 × 10^{-5}	1.35 × 10^{-5}	1.45 × 10^{-5}
	q_e (mg·g^{-1})	609.76	625.01	662.25
	R^2	0.9938	0.9972	0.9955

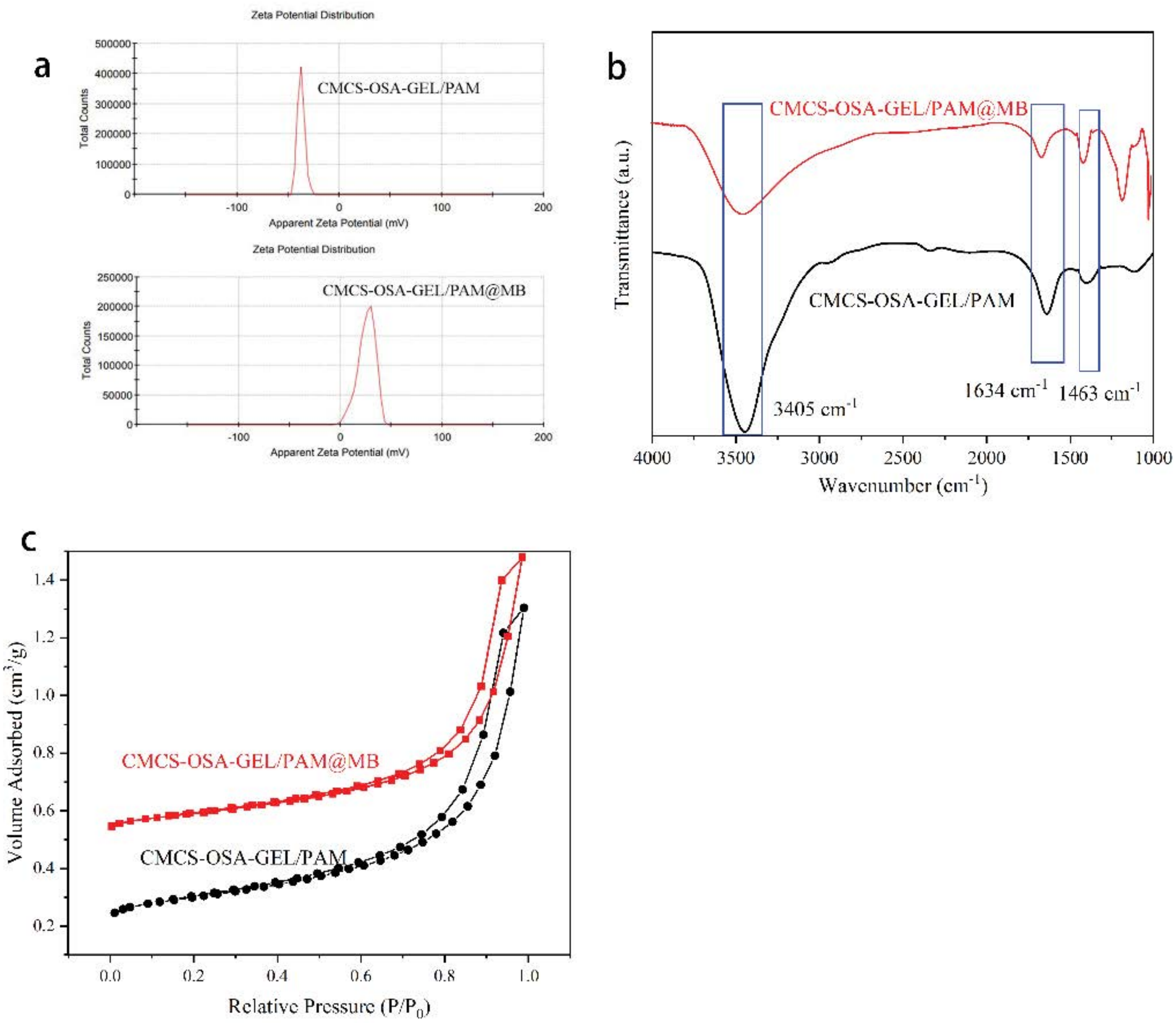

Fig. 6. (a) Zeta potential change before and after adsorption, (b) infrared peak changes before and after hydrogel adsorption, and (c) nitrogen adsorption–desorption isotherm before and after hydrogel adsorption.

4. Conclusion

In this work, a dual network hydrogel (CMCS-OSA-GEL/PAM) of biomass-based polymers and synthetic polymers was prepared by a one-pot method. After the polyacrylamide network was compounded, the hydrogel can withstand a stress of more than 1 MPa, which was twice the stress of the biomass based single network. The adsorption capacity of the CMCS-OSA-GEL/PAM hydrogel can reach 911 mg·g^{-1}, when the methylene blue concentration was 200 mg·L^{-1}. The removal rate of methylene blue by CMCS-OSA-GEL/PAM hydrogel reached more than 93%, and the adsorption rate was still above 86% after 7 adsorption–desorption cycles. CMCS-OSA-GEL/PAM hydrogel with a large number active groups such as carboxyl, amino, hydroxyl, amide, showing satisfactory mechanical property, rich pore structure, cycle stability, which was an excellent adsorbent material for the treatment of dye wastewater.

References

[1] M.A. Granato, T.M. Gaspar, A.F. Alves, A.A.U. de Souza, S. de Souza, Reuse of wastewaters on dyeing of polyester fabric with encapsulated disperse dye, Environ. Technol., 40 (2019) 408–417.

[2] H.B. Madalosso, R.D. Silva, A. Merlini, R. Battisti, R.A.F. Machado, C. Marangoni, Modeling and experimental validation of direct contact membrane distillation applied to synthetic dye solutions, J. Chem. Technol. Biotechnol., 96 (2021) 909–922.

[3] A. Buthiyappan, R. Shah, A. Asghar, A.A.A. Raman, M.A.W. Daud, S. Ibrahim, F.H. Tezel, Textile wastewater treatment efficiency by Fenton oxidation with integration of membrane separation system, Chem. Eng. Commun., 206 (2019) 541–557.

[4] C.D. Raman, S. Kanmani, Textile dye degradation using nano zero valent iron: a review, J. Environ. Manage., 177 (2016) 341–355.

[5] L.H. Ahlstrom, C.S. Eskilsson, E. Bjorklund, Determination of banned azo dyes in consumer goods, TrAC, Trends Anal. Chem., 24 (2005) 49–56.

[6] A.M. Ferreira, A.I. Valente, L.S. Castro, J.A.P. Coutinho, M.G. Freire, A.P.M. Tavares, Sustainable liquid supports for laccase immobilization and reuse: degradation of dyes in aqueous biphasic systems, Biotechnol. Bioeng., 118 (2021) 2514–2523.

[7] A. Kolodziejczak-Radzimska, L.D. Nghiem, T. Jesionowski, Functionalized materials as a versatile platform for enzyme immobilization in wastewater treatment, Curr. Pollut. Rep., 7 (2021) 263–276.

[8] W. Li, B.N. Mu, Y.Q. Yang, Feasibility of industrial-scale treatment of dye wastewater via bio-adsorption technology, Bioresour. Technol., 277 (2019) 157–170.

[9] P. Moradihamedani, Recent advances in dye removal from wastewater by membrane technology: a review, Polym. Bull., 79 (2022) 2603–2631.

[10] J.J. Lu, Y.H. Gu, Y. Chen, X. Yan, Y.J. Guo, W.Z. Lang, Ultrahigh permeability of graphene-based membranes by adjusting D-spacing with poly(ethylene imine) for the separation of dye wastewater, Sep. Purif. Technol., 210 (2019) 737–745.

[11] W.H. Sun, D.F. Liu, M.H. Zhang, Application of electrode materials and catalysts in electrocatalytic treatment of dye wastewater, Front. Chem. Sci. Eng., 15 (2021) 1427–1443.

[12] S. Tunc, T. Gurkan, O. Duman, On-line spectrophotometric method for the determination of optimum operation parameters on the decolorization of Acid Red 66 and Direct Blue 71 from aqueous solution by Fenton process, Chem. Eng. J., 181 (2012) 431–442.

[13] S. Tunc, O. Duman, T. Gurkan, Monitoring the decolorization of Acid Orange 8 and Acid Red 44 from aqueous solution using Fenton's reagents by online spectrophotometric method: effect of operation parameters and kinetic study, Ind. Eng. Chem. Res., 52 (2013) 1414–1425.

[14] M. Akter, M. Bhattacharjee, A.K. Dhar, F.B. Rahman, S. Haque, T.U. Rashid, S.M.F. Kabir, Cellulose-based hydrogels for wastewater treatment: a concise review, Gels, 7 (2021) 30, doi: 10.3390/gels7010030.

[15] H. Mittal, A. Maity, S.S. Ray, Effective removal of cationic dyes from aqueous solution using gum ghatti-based biodegradable hydrogel, Int. J. Biol. Macromol., 79 (2015) 8–20.

[16] S. Lapwanit, T. Sooksimuang, T. Trakulsujaritchok, Adsorptive removal of cationic methylene blue dye by kappa-carrageenan/poly(glycidyl methacrylate) hydrogel beads: preparation and characterization, J. Environ. Chem. Eng., 6 (2018) 6221–6230.

[17] T. Hu, Q.Z. Liu, T.T. Gao, K.J. Dong, G. Wei, J.S. Yao, Facile preparation of tannic acid-poly(vinyl alcohol)/sodium alginate hydrogel beads for methylene blue removal from simulated solution, ACS Omega, 3 (2018) 7523–7531.

[18] L.M. Zhang, Y.J. Zhou, Y. Wang, Novel hydrogel composite for the removal of water-soluble cationic dye, J. Chem. Technol. Biotechnol., 81 (2006) 799–804.

[19] Q. Liu, N. Xia, W.J. Wan, Y.C. Gao, S.M. Zhu, Selective capture of toxic anionic dyes of a novel prepared DMDAAC-grafted chitosan/genipin/cellulose hydrogel beads with antibacterial activity, Int. J. Biol. Macromol., 189 (2021) 722–733.

[20] J. Ren, M. Li, X.M. Wang, R.R. Li, H.T. Wang, W. Yang, Adsorption behaviors of dyes on a biodegradable gelatin/chitosan/beta-cyclodextrin hydrogel from an aqueous solution, Colloid. Polym. Sci., 300 (2022) 785–800.

[21] W. Wang, J.J. Hu, R.D. Zhang, C. Yan, L. Cui, J.J. Zhu, A pH-responsive carboxymethyl cellulose/chitosan hydrogel for adsorption and desorption of anionic and cationic dyes, Cellulose, 28 (2021) 897–909.

[22] J.F. Shi, H. Zhang, Y. Yu, M. Yan, L.W. Liu, H.T. Zhu, Y.M. Ye, Y.H. Zhao, J. Guo, Preparation and adsorption properties of magnetic composite microspheres containing metal-organic double network structure, J. Inorg. Organomet. Polym., 30 (2020) 2301–2314.

[23] T. Chen, H.C. Liu, J. Gao, G.W. Hu, Y. Zhao, X.Q. Tang, X.B. Han, Efficient removal of methylene blue by bio-based sodium alginate/lignin composite hydrogel beads, Polymers, 14 (2022) 2917, doi: 10.3390/polym14142917.

[24] A. Kausar, S.U. Rehman, F. Khalid, A. Bonilla-Petriciolet, D.I. Mendoza-Castillo, H.N. Bhatti, S.M. Ibrahim, M. Iqbal, Cellulose, clay and sodium alginate composites for the removal of methylene blue dye: experimental and DFT studies, Int. J. Biol. Macromol., 209 (2022) 576–585.

[25] X. Wang, H. Zhang, Q.D. He, H.F. Xing, K. Feng, F. Guo, W.B. Wang, Core-shell alginate beads as green reactor to synthesize grafted composite beads to efficiently boost single/co-adsorption of dyes and Pb(II), Int. J. Biol. Macromol., 206 (2022) 10–20.

[26] R. Soury, M. Jabli, S. Latif, K.M. Alenezi, M. El Oudi, F. Abdulaziz, S. Teka, H. El Moll, A. Haque, Synthesis and characterization of a new meso-tetrakis (2,4,6-trimethylphenyl) porphyrinto) zinc(II) supported sodium alginate gel beads for improved adsorption of methylene blue dye, Int. J. Biol. Macromol., 202 (2022) 161–176.

[27] S. Kondaveeti, D.F.S. Petri, H.E. Jeong, Efficiency of air-dried and freeze-dried alginate/xanthan beads in batch, recirculating and column adsorption processes, Int. J. Biol. Macromol., 204 (2022) 345–355.

[28] N.M. Hu, D. Chen, Q.Q. Guan, L.C. Peng, J.H. Zhang, L. He, Y.Z. Shi, Preparation of hemicellulose-based hydrogels from biomass refining industrial effluent for effective removal of methylene blue dye, Environ. Technol., 43 (2022) 489–499.

[29] S.X. Wei, W. Chen, Z.M. Tong, N. Jiang, M.J. Zhu, Synthesis of a functional biomass lignin-based hydrogel with high swelling and adsorption capability towards Acid Red 73, Environ. Sci. Pollut. Res., 28 (2021) 51306–51320.

[30] M.H. Salim, Z. Kassab, E. Ablouh, H. Sehaqui, A. Aboulkas, R. Bouhfid, A. Qaiss, M. El Achaby, Manufacturing of macroporous cellulose monolith from green macroalgae and its application for wastewater treatment, Int. J. Biol. Macromol., 200 (2022) 182–192.

[31] S.Q. Huang, L.J. Wu, T.Z. Li, D.Y. Xu, X.L. Lin, C.D. Wu, Facile preparation of biomass lignin-based hydroxyethyl cellulose super-absorbent hydrogel for dye pollutant removal, Int. J. Biol. Macromol., 137 (2019) 939–947.

[32] X.G. Dang, Z.F. Yu, M. Yang, M.W. Woo, Y.Q. Song, X.C.A. Wang, H.J. Zhang, Sustainable electrochemical synthesis of natural starch-based biomass adsorbent with ultrahigh adsorption capacity for Cr(VI) and dyes removal, Sep. Purif. Technol., 288 (2022) 120668, doi: 10.1016/j.seppur.2022.120668.

[33] X.W. Xu, V.V. Jerca, R. Hoogenboom, Bioinspired double network hydrogels: from covalent double network hydrogels via hybrid double network hydrogels to physical double network hydrogels, Mater. Horiz., 8 (2021) 1173–1188.

[34] R. Zhang, H.W. Peng, T.X. Zhou, M. Li, X.H. Guo, Y. Yao, Selective adsorption and separation of organic dyes by poly(acrylic acid) hydrogels formed with spherical polymer brushes and chitosan, Aust. J. Chem., 71 (2018) 846–854.

[35] N. Naseri, B. Deepa, A.P. Mathew, K. Oksman, L. Girandon, Nanocellulose-based interpenetrating polymer network (IPN) hydrogels for cartilage applications, Biomacromolecules, 17 (2016) 3714–3723.

[36] K. Gayathri, N. Palanisamy, Methylene blue adsorption onto an eco-friendly modified polyacrylamide/graphite composites: investigation of kinetics, equilibrium, and thermodynamic studies, Sep. Sci. Technol., 55 (2020) 266–277.

[37] T. Yao, S. Guo, C.F. Zeng, C.Q. Wang, L.X. Zhang, Investigation on efficient adsorption of cationic dyes on porous magnetic polyacrylamide microspheres, J. Hazard. Mater., 292 (2015) 90–97.

[38] P. Maijan, K. Junlapong, J. Arayaphan, C. Khaokong, S. Chantarak, Synthesis and characterization of highly elastic superabsorbent natural rubber/polyacrylamide hydrogel, Polym. Degrad. Stab., 186 (2021) 109499, doi: 10.1016/j.polymdegradstab.2021.109499.

[39] T. Chen, Y.J. Chen, H.U. Rehman, Z. Chen, Z. Yang, M. Wang, H. Li, H.Z. Liu, Ultratough, self-healing, and tissue-adhesive hydrogel for wound dressing, ACS Appl. Mater. Interfaces, 10 (2018) 33523–33531.

[40] H. Li, D.Z. Hao, J.B. Fan, S.F. Song, X.L. Guo, W.L. Song, M.J. Liu, L. Jiang, A robust double-network hydrogel with under sea water superoleophobicity fabricated via one-pot, one-step reaction, J. Mater. Chem. B, 4 (2016) 4662–4666.

[41] N.F. Alharby, R.S. Almutairi, N.A. Mohamed, Adsorption behavior of Methylene blue dye by novel cross-linked *O*-CM-chitosan hydrogel in aqueous solution: kinetics, isotherm and thermodynamics, Polymers, 13 (2021) 3659, doi: 10.3390/polym13213659.

[42] J.Y. Cao, L. Xiao, X.W. Shi, Injectable drug-loaded polysaccharide hybrid hydrogels for hemostasis, RSC Adv., 9 (2019) 36858–36866.

[43] H.F. Ji, X. Song, H.T. Cheng, L.B. Luo, J.B. Huang, C. He, J.R. Yin, W.F. Zhao, L. Qiu, C.S. Zhao, Biocompatible *in-situ* polymerization of multipurpose polyacrylamide-based hydrogels on skin via silver ion catalyzation, ACS Appl. Mater. Interfaces, 12 (2020) 31079–31089.

[44] M.C. Carre, C. Delestre, P. Hubert, E. Dellacherie, Covalent coupling of a short polyether on sodium alginate-synthesis and characterization of the resulting amphiphilic derivative, Carbohydr. Polym., 16 (1991) 367–379.

[45] O. Ismail, O.G. Kocabay, Absorption and adsorption studies of polyacrylamide/sodium alginate hydrogels, Colloid. Polym. Sci., 299 (2021) 783–796.

[46] Y.Y. Yue, X.H. Wang, J.Q. Han, L. Yu, J.Q. Chen, Q.L. Wu, J.C. Jiang, Effects of nanocellulose on sodium alginate/polyacrylamide hydrogel: mechanical properties and adsorption–desorption capacities, Carbohydr. Polym., 206 (2019) 289–301.

[47] M.N. Zafar, Q. Dar, F. Nawaz, M.N. Zafar, M. Igbal, M.F. Nazar, Effective adsorptive removal of azo dyes over spherical ZnO nanoparticles, J. Mater. Res. Technol., 8 (2019) 713–725.

[48] I. Ghosh, S. Kar, T. Chatterjee, N. Bar, S.K. Das, Removal of methylene blue from aqueous solution using *Lathyrus sativus* husk: adsorption study, MPR and ANN modelling, Process Saf. Environ. Prot., 149 (2021) 345–361.

[49] H. Ge, H.L. Huang, M. Xu, Q. Chen, Cellulose/poly(ethylene imine) composites as efficient and reusable adsorbents for heavy metal ions, Cellulose, 23 (2016) 2527–2537.

[50] X.Y. Liu, Y.F. Zhou, W.Y. Nie, L.Y. Song, P.P. Chen, Fabrication of hydrogel of hydroxypropyl cellulose (HPC) composited with graphene oxide and its application for methylene blue removal, J. Mater. Sci., 50 (2015) 6113–6123.

[51] O. Duman, S. Tunc, B.K. Bozoglan, T.G. Polat, Removal of triphenylmethane and reactive azo dyes from aqueous solution by magnetic carbon nanotube-κ-carrageenan-Fe_3O_4 nanocomposite, J. Alloys Compd., 687 (2016) 370–383.

[52] O. Duman, S. Tunc, T.G. Polat, Adsorptive removal of triarylmethane dye (Basic Red 9) from aqueous solution by sepiolite as effective and low-cost adsorbent, Microporous Mesoporous Mater., 210 (2015) 176–184.

[53] Y.J. Chang, J.Y. Lai, D.J. Lee, Thermodynamic parameters for adsorption equilibrium of heavy metals and dyes from wastewaters: research updated, Bioresour. Technol., 222 (2016) 513–516.